*Environ. Water Eng., 2025, 11(3), 282-294* https://doi.org/10.22034/ewe.2025.495490.1991

EWE

**Environment and Water Engineering**

**Homepage: www.jewe.ir**

ISSN: 2476-3683

# Green synthesis of a melamine-based MOF and its performance in dye removal

Elham Asadi[1], Fatemeh Abyar[2], and Fatemeh Abrishami[3]

[1]Department of Organic Chemistry, Faculty of Chemistry, Alzahra University, Tehran, Iran
[2]Department of Chemical Engineering, Faculty of Engineering, Ardakan University, P.O. Box 184, Ardakan, Iran
[3]Department of Chemistry, Faculty of Chemistry and Chemical Engineering, Malek-Ashtar University of Technology, Tehran, Iran

**ARTICLE INFO**

**Paper Type:** Research Paper

**Received**: 23 December 2024
**Revised:** 12 April 2025
**Accepted**: 27 April 2025
**Published**: 05 May 2025

**Keywords**
Adsorption
Dye Removal
Environment
Kinetics
Isotherm

**Corresponding authors:**
E.Asadi
✉ E.Asadi@alzahra.ac.ir
F. Abyar
✉ f.abyar@ardakan.ac.ir

**ABSTRACT**

Cationic dyes like methylene blue (MB) and basic red 46 (BR-46) pose significant environmental risks due to their toxicity and persistence in aquatic systems. This study aims to enhance adsorption efficiency by modifying a melamine-based metal-organic framework (MOF). By altering the solvent during synthesis, a porous structure, $[Cu(\eta^1\text{-}OAc)(\mu\text{-}OC_2H_5)(MA)]_2$ (CMP-Et), was successfully derived from $[Cu(\eta^1\text{-}OAc)(\mu\text{-}OCH_3)(MA)]_2$ (CMP-Me) using low-cost ethanol as a green solvent. The materials were characterized using XRD, FT-IR, and SEM. The removal efficiency of MB and BR-46 at an initial concentration of 20 mg/l was found to be 80 and 37%, respectively. The adsorption capacity of CMP-Et for the removal of MB and BR-46 was calculated to be 161 and 74 mg/g, respectively. The adsorption data for these dyes were consistent with the Langmuir and the Freundlich/Temkin isotherms, respectively, and followed pseudo-second-order kinetics. This work demonstrates the potential of cost-effective MOFs synthesized from inexpensive solvents like ethanol for efficient textile wastewater treatment.

**Highlights**

- Cost-effective, scalable synthesis of CMP-Et MOF for efficient dye removal
- Rapid >80% dye removal within 30 minutes
- MB follows Langmuir; BR-46 fits Freundlich/Temkin isotherms
- High adsorption capacity for MB and following pseudo-second-order kinetics

**How to cite this paper:**
Asadi, E., Abyar, F., & Abrishami, F. (2025). Green synthesis of a melamine-based MOF and its performance in dye removal. *Environment and Water Engineering*, *11*(3), 282-294. https://doi.org/10.22034/ewe.2025.495490.1991

## 1. Introduction

Among the most critical issues in industries is the reduction and elimination of pollution and contaminants from wastewater. The wastewater from each industry varies depending on the type of product and the production process in different factories. This wastewater may contain organic matter, dyes, suspended chemical particles, heavy metals, and other pollutants (Deshmukh et al., 2025). The removal of dyes and pigments from wastewater has become a significant concern in recent years. Industries such as textiles, paper manufacturing, printing, plastics, leather, tanning, food, and cosmetics extensively use coloring agents to dye their products (Fattahi et al. 2024). The discharge of colored wastewater from these industries can pose serious environmental hazards(Yin et al., 2019). Annually, approximately 700,000 tons of dyes and pigments, comprising nearly 10,000 different varieties, are produced worldwide (Ashraf et al., 2021). These dyes belong to diverse structural and functional categories, with an estimated 2-26% entering wastewater streams during the dyeing process (Aksu et al. 2010). The discharge of colored effluents from textile industries into receiving water bodies reduces sunlight penetration, deteriorates visual clarity, and disrupts aquatic ecosystems. This phenomenon significantly

impairs photosynthetic activity in aquatic plants and algae, ultimately causing substantial environmental damage (Mahmoodi et al., 2019). Dyes exhibit carcinogenic and mutagenic properties in humans and may cause skin irritation and other dermatological effects. Therefore, efficient and effective treatment of colored wastewater is essential (Kestioğlu et al., 2005). Various treatment techniques are utilized for dye removal from wastewater, including physical adsorption methods such as membrane filtration, surface adsorption, and ion exchange, and chemical treatment approaches including chemical oxidation, advanced oxidation processes (AOPs), and electrocoagulation(N Lotha et al. 2024). Methods such as membrane separation suffer from high maintenance costs and membrane fouling issues. While ion exchange offers high efficiency, it involves expensive resins and sensitivity to interfering ions (Dhokpande et al., 2024). Advanced oxidation processes, including chemical oxidation, provide high degradation rates but come with substantial costs for chemicals, energy, and equipment, along with the risk of generating toxic byproducts. Electrocoagulation, despite its high efficiency, entails significant energy consumption and sludge production. In contrast, adsorption stands out as a simple, cost-effective, and efficient method, making it an ideal choice for removing dyes from wastewater (Hama Aziz et al., 2024). Because this method is a selective process for removing dye from wastewater, it offers the possibility of recycling and reusing the adsorbent and reducing residues from production (Değermenci et al., 2019). Several low-cost, selective, and effective adsorbents have been utilized, including orange peel, banana stem, rice husk, clay, activated carbon, coal ash, sawdust, silica gel, and chitosan (Namasivayam et al., 1996; Sharma et al. 2009). Moreover, multi-walled carbon nanotubes (MWCNTs), Sobhanardakani et al. (2013); Sobhanardakani et al. (2017), $NiFe_2O_4$ nanoparticles, Sobhanardakani et al. (2016); Zandipak et al. (2016), and various metal-organic frameworks (MOFs) and their composites, such as guanidine-functionalized chitosan/UiO-66-$NH_2$ nanohybrid (UiO-66-$NH_2$@Cs-ISo-Gu), are currently being employed and developed. Metal-organic frameworks, as a novel class of advanced nanoporous materials, exhibit wide-ranging applications, particularly in adsorption and separation processes (Asadi et al., 2022). This class of porous compounds has attracted significant attention in adsorption processes due to their large pore sizes, high surface area, selective uptake of small molecules, and optical or magnetic responses in the presence of guest molecules. MOFs are formed through the coordination of metal clusters (as coordination centers) with organic ligands (as metal ion linkers). These compounds possess unique physical and chemical properties(Stavila et al. 2014; Freund et al., 2021). Recently, MOFs have been under development for dye removal from aqueous wastewater (He et al. 2014; Asadi et al. 2022). Compared with other porous adsorbents such as activated carbon and zeolites, MOFs offer numerous advantages, including extremely low density, tunable structure, large active surface area, simple synthesis, and high thermal stability, making them suitable for various physical and chemical applications(Gangu et al., 2016; Wang et al. 2016). Enamul Haque used MOF-235 to remove methylene blue (MB) and methyl orange (MO) dyes from aqueous solutions. According to this study, even if MOFs do not adsorb gases, they can be proposed as potential adsorbents for the removal of harmful substances in the liquid phase. The adsorption of MO and MB at different temperatures indicates that the adsorption process is spontaneous, and entropy increases with the adsorption of MO and MB (Haque et al., 2011). Liu synthesized a polyoxometalate ($H6P_2W_{18}O_{62}$)-based metal-organic framework composite via a simple one-step thermal solvent method and demonstrated its effectiveness as an adsorbent, achieving 80% removal of MB (20 mg/L) within 90 minutes (Liu et al., 2015). Similarly, Li reported that BUC-17 MOF adsorbed 99.1% of Congo red (100 ppm) in just 3 minutes (Li et al., 2017). Complementing these advances, Mahmoodi engineered a graphene oxide-incorporated MOF (NENU/GO) under ambient conditions using ethanol, demonstrating enhanced adsorption of Basic Red 46 (5–20 mg/l) across pH ranges, with π-π interactions identified as the dominant mechanism (Mahmoodi et al. 2019). Building on these findings, this study investigates the efficacy of a novel melamine-based MOF (CMP-Et) for removing two cationic dyes, MB and BR 46, from aqueous solutions. The significance of this research is twofold: First, melamine-based MOFs are particularly valuable for adsorption processes due to the ligand's low cost and high porosity. Second, the framework coordinates with metal ions through melamine's nitrogen atoms while providing three free amine groups. These characteristics enable CMP-Et to achieve rapid, high-capacity adsorption of cationic dyes through combined hydrogen bonding and electrostatic interactions, in addition to its inherent porosity. The study systematically probes CMP-Et's adsorption behavior toward cationic dyes under diverse conditions, offering insights for designing scalable MOF-based solutions for industrial wastewater purification.

## 2. Materials and Methods

### 2.1 Materials and Equipment

MB and BR 46 were used as model contaminants and were purchased from Merck without further purification. Spectral analyses, including FTIR spectra, were performed using a Nicolet 800 spectrometer with KBr tablets, and Ultraviolet–visible spectroscopy was performed using a Hitachi U-3310 spectrometer. In addition, the calculated specific surface area (BET) was obtained using the computational method reported by Tovari, based on the effective area of each methylene blue molecule (Brij and Clint, 2010).

In addition, X-ray diffraction (XRD) analysis was performed using a Stoe MP Stady instrument (STOE & Cie GmbH, Germany), and scanning electron microscopy (SEM) analysis was conducted using a MIRA3 TESCAN device (TESCAN ORSAY HOLDING, Czech Republic).

### 2.2 Synthesis of CMP-Me

CMP-Me was synthesized following a previously reported method (Chen et al., 2006). A mixture of 4 g $Cu(OAc)_2 \cdot H_2O$ (20 mmol) and 2.5 g melamine (20 mmol) was added to 200 ml of methanol. The solution was refluxed for 3 h. After cooling to room temperature, the resulting blue solid was isolated, washed twice with diethyl ether, and dried under vacuum.

### 2.3 Synthesis of CMP-Et

CMP-Et was synthesized following the same procedure as reported for CMP-Me (Chen et al., 2006), with the only

modification being the use of ethanol instead of methanol as the solvent. Accordingly, a mixture of 2.5 g melamine (20 mmol) and 4 g $Cu(OAc)_2 \cdot H_2O$ (20 mmol) in 200 ml ethanol was refluxed for 3 h. After cooling to room temperature, the resulting green solid was isolated, washed twice with diethyl ether, and dried under vacuum.

### 2.4 Ultrasonic Adsorption Method

Dye adsorption in batch mode was carried out in an ultrasonic bath (frequency: 30 kHz, power: 200 W). Pollutant removal experiments were performed by mixing varying amounts of adsorbent (0.004, 0.006, 0.008, and 0.01 g) with 100 ml of dye solution (20 mg/l) at natural pH 6. The effect of adsorbent dosage on the removal of two cationic dyes was investigated. After the adsorption process, the adsorbent particles were separated from the solution samples via centrifugation. The residual concentrations of MB and BR-46 were measured using a UV-Vis spectrophotometer at wavelengths of 665 nm and 531 nm, respectively. Adsorption kinetics and isotherms were studied for both dyes (20 mg/l, pH 6) at varying adsorbent dosages. All dye removal experiments were conducted in triplicate, with an experimental error of approximately 3%.

## 3. Results and Discussion

This study presents a novel synthetic route for preparing a copper-melamine supramolecular framework (CMP-Et) with enhanced dye removal properties. Unlike the previously reported CMP-Me structure (Chen et al. 2006), which was synthesized using methanol as the solvent and auxiliary ligand, CMP-Et was independently prepared under identical conditions but with ethanol replacing methanol during the initial synthesis. This solvent substitution led to the formation of a distinct green-phase material (CMP-Et) with modified structural and functional properties.

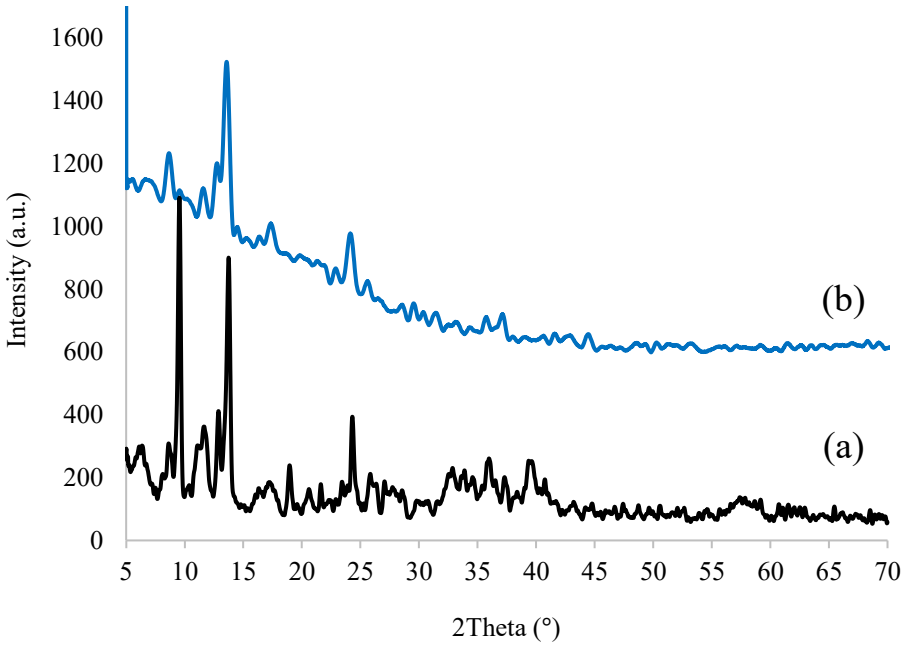


**Fig. 1** X-ray diffraction pattern of the MOFs: a) CMP-Me and b) CMP-Et

### 3.1 CMP-Et Characterization Results

XRD patterns of CMP-Me and CMP-Et, shown in Fig. 1a and 1b, respectively, reveal sharp peaks at 2$\theta$ of 9.5, 11.7, 13.7, and 24.3° in both structures, indicating shared crystalline features. However, observed differences in other regions of the XRD patterns -particularly in peak positions and intensities- highlight the impact of solvent change (from methanol to ethanol) and the role of the auxiliary ligand in inducing structural modifications. These changes led to the formation of a new crystalline structure in CMP-Et, which, despite overall similarities, differs from CMP-Me in crystalline arrangement and lattice parameters. In previous studies, the XRD pattern of the CMP-Me structure was not reported (Chen et al., 2006). Nonetheless, a comparison of these two MOFs confirms the emergence of a new crystalline structure in CMP-Et, attributed to structural alterations caused by the solvent acting as an auxiliary ligand(Qin et al., 2012; Qin et al., 2014).

The FT-IR spectrum of CMP-Et is shown in Fig. 2. The C-H bending vibration related to ethanol at 1465 $cm^{-1}$, the C-O stretching vibration at 1028 $cm^{-1}$, and the Cu-O stretching vibration at 554 $cm^{-1}$ confirm the presence of solvent as an auxiliary ligand in the structure (George et al. 1998; Asadi et al. 2025). The primary amine stretching vibrations in the range 3472-3249 $cm^{-1}$ confirm the non-coordination of copper with $NH_2$ groups of melamine. The C=N···Cu stretching vibration and Cu-N vibration at 1624 $cm^{-1}$ and 443 $cm^{-1}$, respectively, indicate the coordination of Cu with triazine nitrogens. The N-H bending vibration at 1549 $cm^{-1}$ and aromatic C-N stretching at 1439 $cm^{-1}$ confirm the presence of melamine in the MOF structure (Chen et al., 2006).

The surface morphology of CMP-Et, examined by SEM at 2 µm magnification, reveals the formation of faceted polyhedral crystals (Fig. 3). The faceted polygonal shape of the crystals indicates the presence of distinct and regular crystal planes, which is consistent with the XRD results. Studies have shown that different solvents can influence crystal growth rates and

the orientation of crystalline planes, leading to the formation of various crystal morphologies(Qin et al., 2012; Qin et al., 2014).

**Fig. 2** FT-IR spectrum of the CMP-Et framework

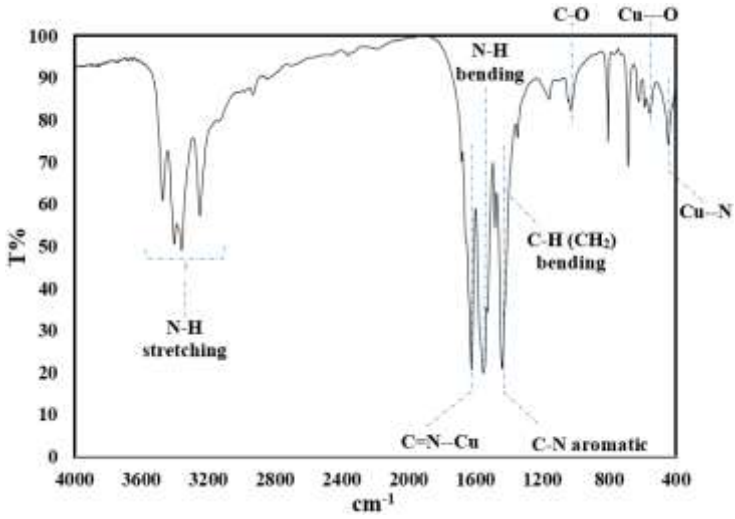


**Fig. 3** Both images a) and b) SEM of the CMP-Et framework:

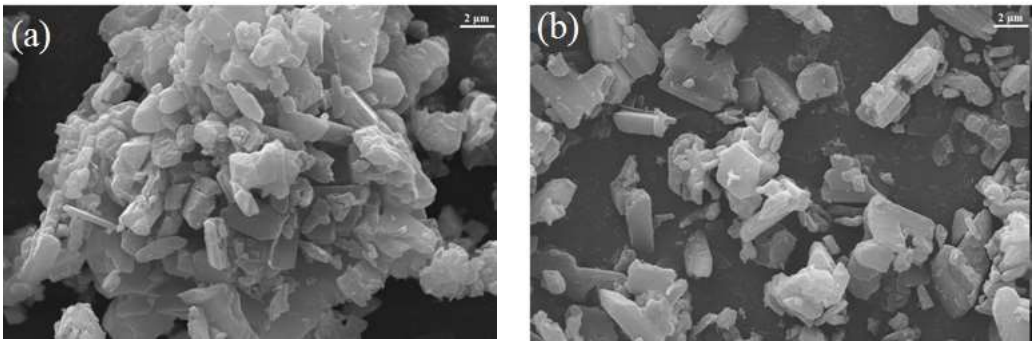


The results of inductively coupled plasma spectrometry (ICP) analysis revealed a copper weight percentage of 20.2 ± 0.2% in the CMP-Et structure. For determining the active surface area of CMP-Et, the computational method reported by Tewari in Eq. 1 was employed (Brij and Clint, 2010). Assuming an effective area of 130 $Å^2$ per methylene blue molecule, the specific surface area of the metal-organic framework was calculated to be 560.2 $m^2/g$ (Eq. 1), where $Q_{monolayer}$ represents the maximum adsorption capacity derived from the Langmuir isotherm model.

$$A = Q_{monolayer}/M_w \times 6.022 \times 10^{23} \times A \text{ (molecular)} \quad (1)$$

### 3.2 Adsorption studies

The results of the removal efficiency variations for MB and BR-46 by the CMP-Et adsorbent are presented in Fig. 4(a,b). For dye solutions with an initial concentration of 20 mg/l, increasing the CMP-Et adsorbent dosage from 0.004 to 0.01 g led to enhanced adsorption of both dyes. This improvement is attributed to the increased accessibility of active adsorption sites on the adsorbent surface (Moradi et al. 2022). The maximum adsorption capacity was observed at an adsorbent dosage of 0.01 g, as this quantity provides the highest number of available active sites for dye molecule adsorption (Asadi et al., 2022).

The specific surface area is a key parameter determining the adsorption capacity of materials. Higher specific surface area leads to increased porosity and contact surface with adsorbate molecules, resulting in enhanced adsorption performance (Majd et al. 2022). The results demonstrated that the CMP-Et adsorbent exhibited superior performance in removing cationic MB (80.39%) compared with BR 46 (37.01%) from aqueous solutions. This significant difference can be attributed to the chemical structure and particle size of the dyes. Due to its smaller molecular size and more favorable chemical structure, MB demonstrates better penetration into the adsorbent's pores (Hor et al., 2016).

The adsorption time is also one of the important factors in the adsorption process. The shorter adsorption time indicates high porosity and the presence of surface load against absorbent molecules. This characteristic is particularly advantageous for water treatment systems in terms of processing time and economic efficiency (Asadi et al. 2022). In this study, 79% of MB and 36% of BR-46 (20 mg/l) were removed within the first 30 min after adding 0.01 g of the adsorbent. These results demonstrate that CMP-Et is particularly effective for the rapid removal of cationic dyes such as methylene blue.

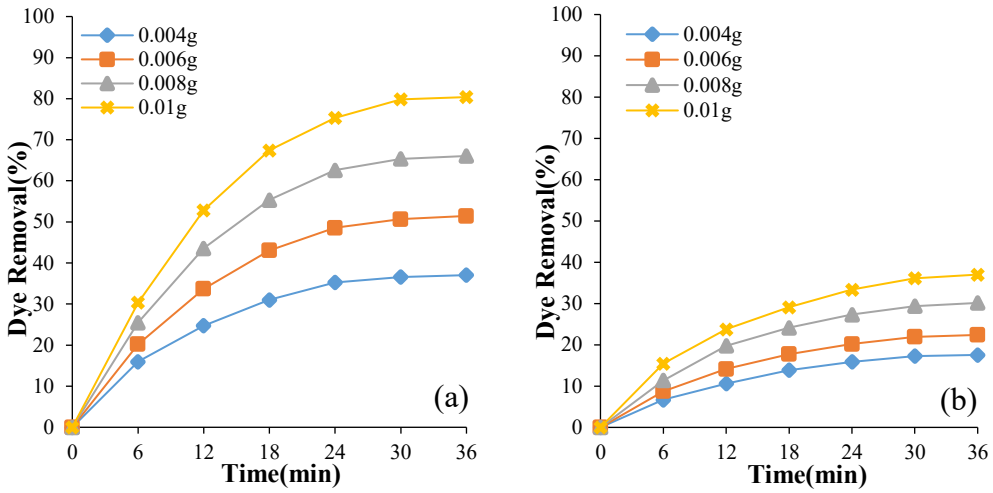


**Fig. 4** Dye removal (%) of: a) MB and b) BR-46 versus CMP-Et adsorbent dosage (dye concentration: 20 ppm; contact time: 6-36 min)

Fig. 5 (a and b) illustrates the adsorption capacity of CMP-Et (0.004-0.01 g) for (a) MB and (b) BR-46 removal at an initial dye concentration of 20 mg/L (contact time: 6-36 min). The adsorption capacity analysis revealed that CMP-Et exhibited superior performance in MB removal with an adsorption capacity of 160.79 mg/g, compared with 74.02 mg/g for BR-46. This difference in adsorption capacity may be attributed to the distinct chemical structures of the two dyes and their varying interactions with the adsorbent surface. Due to its planar molecular structure and positive charge, MB likely forms stronger interactions, such as electrostatic and hydrogen bonds, with the functional groups present in the CMP-Et structure (Asadi et al. 2022).

The highest adsorption capacity was achieved with 0.004 g of the adsorbent for MB removal. Increasing the adsorbent dosage from 0.004 to 0.01 g resulted in a decline in adsorption capacity for both dyes, likely due to the saturation of active adsorption sites and reduced accessibility to these sites at higher adsorbent quantities(Khamizov, 2020).

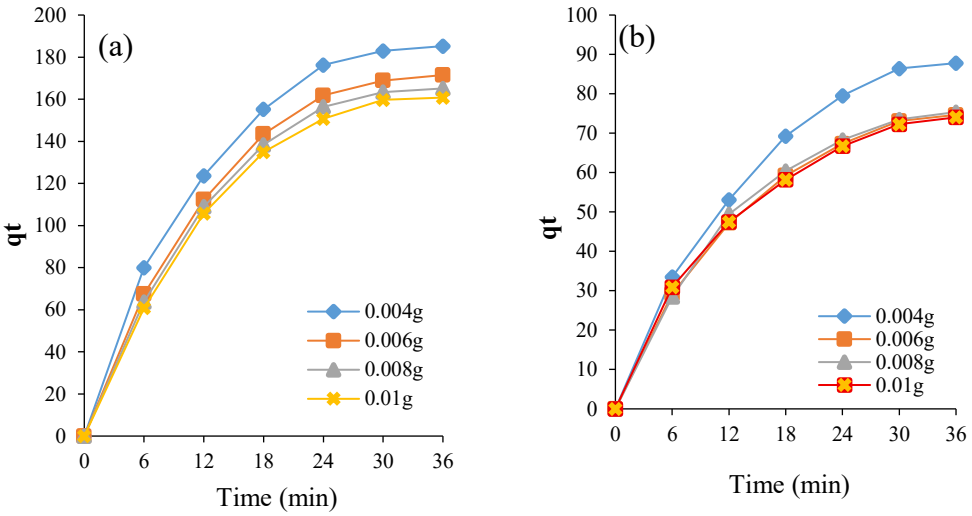


**Fig. 5** The adsorption capacity of: a) MB and b) BR-46 versus CMP-Et adsorbent dosage (dye concentration: 20 ppm; contact time: 6-36 min)

Table 1 compares the adsorption capacities of various MOFs for MB removal, showing that CMP-Et exhibits superior performance with an adsorption capacity of 161 mg/g compared with well-known MOFs such as Cu-BTC (96.4 mg/g), UiO-66 (107 mg/g), and $\{[Cu(L)(H_2O)](DMF)\}_n$ (143.3 mg/g). This enhanced performance is attributed to CMP-Et's high specific surface area, optimal porosity, and active functional groups that promote stronger interactions with MB molecules. However, CMP-Et demonstrates lower adsorption capacity than IFMC-1 (293.9 mg/g) and $[ZnBT(H_2O)_2]_n$ (458.24 mg/g), which is explained by their higher nitrogen content and stronger electrostatic attraction, enabling more robust interactions with MB molecules.

### 3.2.1 Kinetics Studies

In adsorption processes, first-order and second-order kinetic models are employed to describe adsorption rates and predict system behavior (Azizian et al. 2021). The pseudo-first-order kinetic model, introduced by Lagergren in 1898 (Eq. 2), expresses the adsorption process where $q_e$ and $q_t$ represent the amount of adsorbed substance per unit mass of adsorbent at equilibrium and at time t, respectively, and $K_1$ is the pseudo-first-order adsorption rate constant(Pascu et al. 2013). The pseudo-second-order kinetic model, developed by Blanchard in 1984 (Eq. 3), determines the pseudo-second-order rate constant ($K_2$) and adsorption capacity ($q_e$) from the slope and intercept of the corresponding plot(Oboh et al. 2013). These models are widely used to study the adsorption of various substances, including metal ions, dyes, and organic

compounds from aqueous solutions, serving as essential tools for designing and optimizing adsorption systems.

**Table 1** Comparison of methylene blue adsorption capacity with different MOFs

| Entry | MOFs | Adsorption capacity (mg/g) | Ref. |
|---|---|---|---|
| 1 | $[(CH_3)_2NH_2][In(L)]\cdot 4H_2O\cdot 2DMF$ | 281 | Azhar et al. (2017) |
| 2 | Cu-BTC | 96.4 | Kaur et al. (2019) |
| 3 | UiO-66 | 107 | Liu et al. (2019) |
| 4 | HKUST-1 | 454 | Liu et al. (2019) |
| 5 | $[ZnBT(H_2O)_2]_n$ | 458.24 | Asadi et al. (2022a) |
| 6 | IFMC-1 | 293.9 | Asadi et al. (2022b) |
| 7 | $\{[Cu(L)(H_2O)](DMF)\}_n$ | 143.3 | Li et al. (2024) |
| 8 | CMP-Et | 185.25 | This study |

$$log(q_e-q_t)=logq_e-(K_1/2.303)t \quad (1)$$

$$t/q_t=(1/K_2\, q_e^2)+(t/q_e) \quad (2)$$

The kinetic results of the removal of methylene blue and basic red 46 dyes at a concentration of 20 mg/l in the presence of porous CMP-Et adsorbent, with different amounts of adsorbent and different contact times, are shown in Fig. 6.

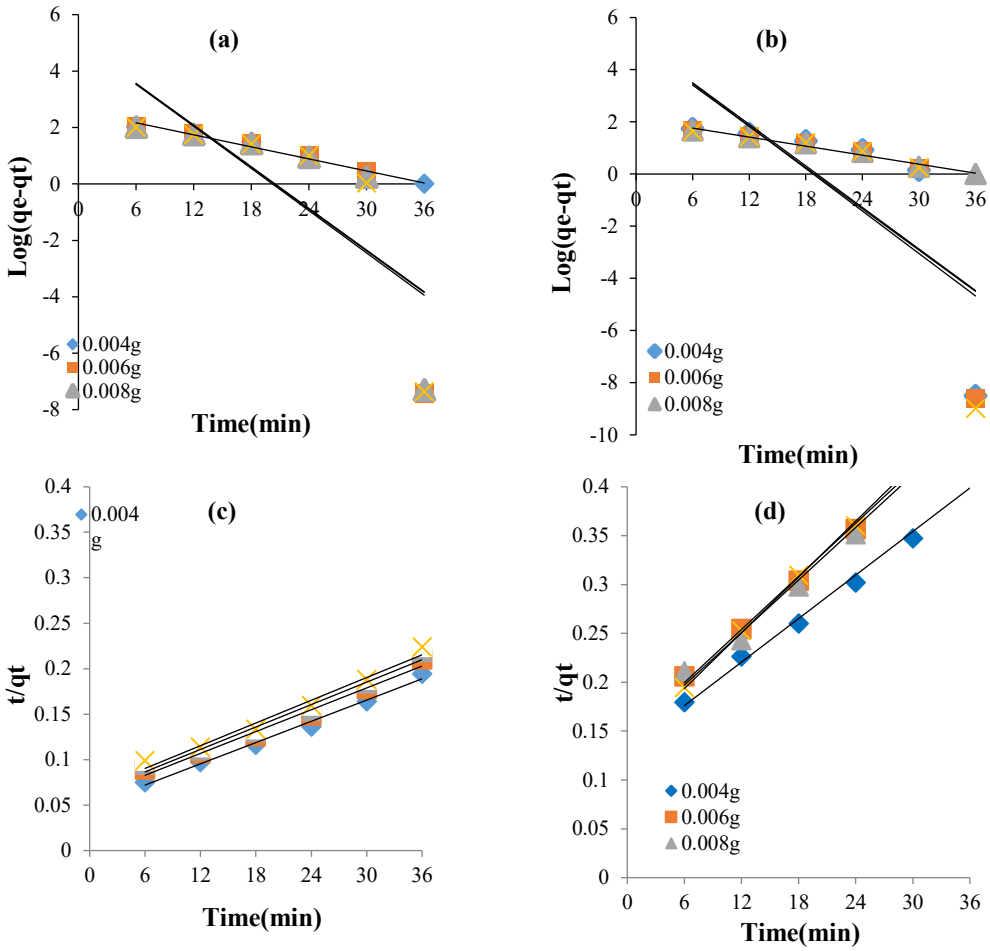


**Fig. 6** Kinetics of pseudo-first order: a) MB, b) BR-46, pseudo-second order: c) MB, d) BR-46 (20 ppm) by CMP-Et adsorbent; contact time: 6-36 min

The kinetic results showed that the adsorption process followed a pseudo-second-order kinetic model, while the experimental data were in poor agreement with the pseudo-first-order model and did not show a suitable correlation coefficient as shown in Fig. 6 (a and b). The good fitness of the data to the pseudo-second-order model (with a high correlation coefficient) suggests that the adsorption mechanism is mainly controlled by chemical interactions between the dye molecules and the active sites of the adsorbent (Bullen et al. 2021) as shown in Fig. 6 (c and d). These results confirm that the adsorption of dyes on CMP-Et occurs through electrostatic bonds, hydrogen bonding, or π-π interactions, and the adsorption capacity depends on the amount of active sites on the adsorbent surface(Khamizov, 2020).

The results demonstrate that the pseudo-second-order model more accurately describes the adsorption process, emphasizing the importance of chemical interactions in adsorption. The experimental and calculated $q_e$ values, rate constants, correlation coefficients for both pseudo-first-order and pseudo-second-order kinetic models, along with the intra-particle diffusion constant ($K_{diff}$), are presented in Table 2 These results indicate that the adsorption of MB and BR-46 onto CMP-Et is primarily controlled by intra-particle diffusion. However, comparison of the correlation coefficients ($R^2$) for the pseudo-first-order and pseudo-second-order kinetic models reveals that the pseudo-second-order model shows better agreement with the experimental data, confirming the significant role of chemical interactions in the adsorption process (Ho 2006).

**Table 2** The kinetics and intraparticle diffusion constants of MB and BR-46 adsorption by CMP-Et

| Adsorbent | | Pseudo-first order | | | Pseudo-second order | | | Intraparticle diffusion | | |
|---|---|---|---|---|---|---|---|---|---|---|
| CMP-Et | | $\log(q_e-q_t) = \log(q_e) - (K_1/2.303)\ t$ | | | $(t/q_t) = (1/K_2\ q_e^2) + (1/q_e)t$ | | | $qt= K_{diff}\ t^{1/2} + I$ | | |
| Dosage | $q_e$(exp) | $q_e$(cal) | $k_1$ | $R^2$ | $q_e$(cal) | $k_2$ | $R^2$ | $k_{diff}$ | I | $R_2$ |
| (g) | (mg/g) | (mg/g) | | | (mg/g) | | | (mg/g $min^{1/2}$) | (mg/g) | |
| **MB-20 (mg/l)** | | | | | | | | | | |
| 0.004 | 185.2495 | 391.7419 | 0.16351 | 0.979 | 333.333 | 0.00019 | 0.99 | 30.6 | 15.23 | 0.939 |
| 0.006 | 171.5039 | 109395.6 | 0.56654 | 0.584 | 250 | 0.00028 | 0.984 | 29.92 | 5.24 | 0.935 |
| 0.008 | 165.1355 | 100925.3 | 0.56424 | 0.6 | 250 | 0.00026 | 0.98 | 29.14 | 3.808 | 0.93 |
| 0.01 | 160.7898 | 110917.5 | 0.57345 | 0.611 | 250 | 0.00025 | 0.978 | 28.69 | 1.864 | 0.932 |
| **BR46-20 (mg/l)** | | | | | | | | | | |
| 0.004 | 87.79273 | 123310.5 | 0.6103 | 0.563 | 142.857 | 0.00037 | 0.991 | 15.95 | -2.294 | 0.968 |
| 0.006 | 74.64633 | 97949 | 0.60569 | 0.552 | 111.111 | 0.00056 | 0.995 | 13.11 | 0.464 | 0.966 |
| 0.008 | 75.36563 | 127.9381 | 0.13127 | 0.978 | 111.111 | 0.00057 | 0.99 | 13.23 | 0.718 | 0.954 |
| 0.01 | 74.0201 | 124451.5 | 0.62411 | 0.542 | 111.111 | 0.0006 | 0.997 | 12.45 | 3.178 | 0.973 |

### 3.2.2 Adsorption Mechanism

In this study, the intra-particle diffusion model (Eq. 4) was employed to examine the adsorption mechanism and identify the rate-limiting step, where $q_t$ represents the adsorption capacity at time t, $K_{diff}$ denotes the intra-particle diffusion rate constant, and I is a constant related to the boundary layer thickness (Mahmoodi et al. 2019).

$$q_t = K_{diff} t^{1/2} + I \quad (4)$$

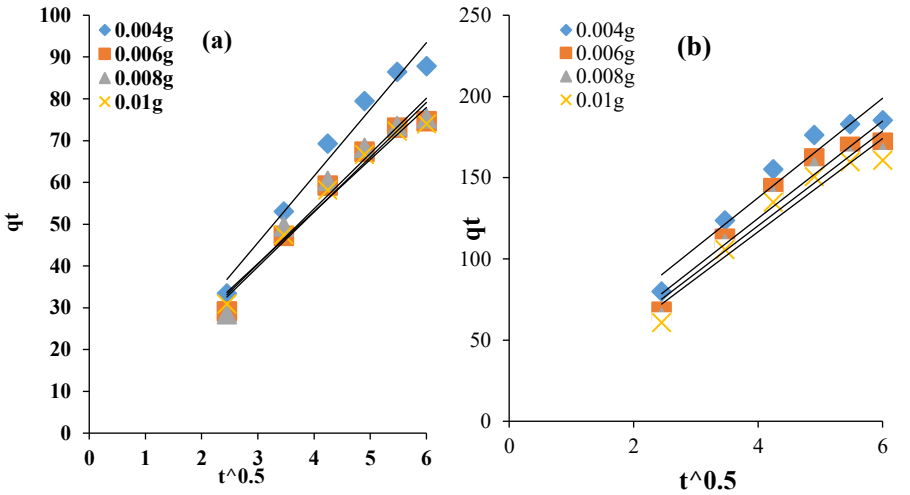


**Fig. 7** Intraparticle diffusion of a) MB and b) BR-46 sorption (20ppm) by the CMP-Et adsorbent

The boundary layer diffusion model was evaluated for the adsorption of cationic dyes (20 mg/L) using CMP-Et at various adsorbent dosages (0.004, 0.006, 0.008, and 0.01 g) and contact times (6-36 min) (Fig. 7 (a,b)). The high correlation coefficients and linear trends under all experimental conditions confirm that boundary layer diffusion is the rate-limiting step for both methylene blue and Basic Red 46 adsorption onto CMP-Et, indicating the adsorption process is predominantly controlled by mass transfer through the boundary layer and intra-particle diffusion (Dharmarathna et al., 2024).

### 3.2.3 Isotherm Studies

Adsorption isotherm models were employed to describe the adsorption behavior of various materials. These models

establish the relationship between the amount of adsorbed substance on the adsorbent surface (q) and its concentration in the liquid phase (C) at equilibrium. In this study, three adsorption isotherm models were investigated: Langmuir, Freundlich, and Temkin.

The Langmuir isotherm model is based on the assumptions of monolayer adsorption on a uniform surface without interactions between adsorbed molecules(Ghasemzadeh et al. 2025). This model is expressed by Eq. 5, where $q_e$ (mg/g) is the amount of adsorbed dye at equilibrium, $q_{max}$ (mg/g) is the monolayer adsorption capacity (maximum amount of adsorbed dye), $K_L$ (l/mg) is the Langmuir equilibrium constant (related to adsorption free energy and adsorbent-adsorbate affinity), and $C_e$ (mg/l) is the equilibrium concentration of the adsorbate (El Jery et al., 2024).

$$C_e/q_e=(1/K_L\ Q_{max})+(1/Q_{max})C_e \quad (5)$$

The Freundlich isotherm describes adsorption on heterogeneous surfaces with non-uniform adsorption energies and is expressed by Eq. 6, where $K_F$ is the Freundlich constant and 1/n represents the adsorption intensity or surface heterogeneity (El Jery et al., 2024).

$$Logq_e= LogK_F + (1/n)\ LogC_e \quad (6)$$

The Temkin isotherm assumes that adsorption energy decreases linearly with surface coverage, making it ideal for modeling chemisorption on heterogeneous surfaces. Its key feature is the linear decline in adsorption energy as coverage increases. The model calculations are performed using Eq. 7 (Mahmoodi et al., 2019).

$$q_e= B_T\ LnK_T + B_T\ LnC_e \quad (7)$$

The experimental results obtained from various tests were fitted to Langmuir, Freundlich, and Temkin isotherm equations. From the Langmuir plots (Fig. 8a (MB) and 8d (BR-46)), the constants $K_L$ and $q_{max}$ were determined. The Freundlich plots (Fig. (8b (MB) and 8e (BR-46))) yielded the constants 1/n and $K_F$, while the Temkin plots (Fig. (8c (MB) and 8f (BR-46))) provided the constants $K_T$ and $B_T$.

**Fig. 8:** a) The Langmuir, b) Freundlich, and c) Temkin isotherm plots of MB adsorption, and the d) Langmuir, e) Freundlich, and f) Temkin isotherm plots for BR-46 sorption (20 ppm) by CMP-Et metal-organic framework

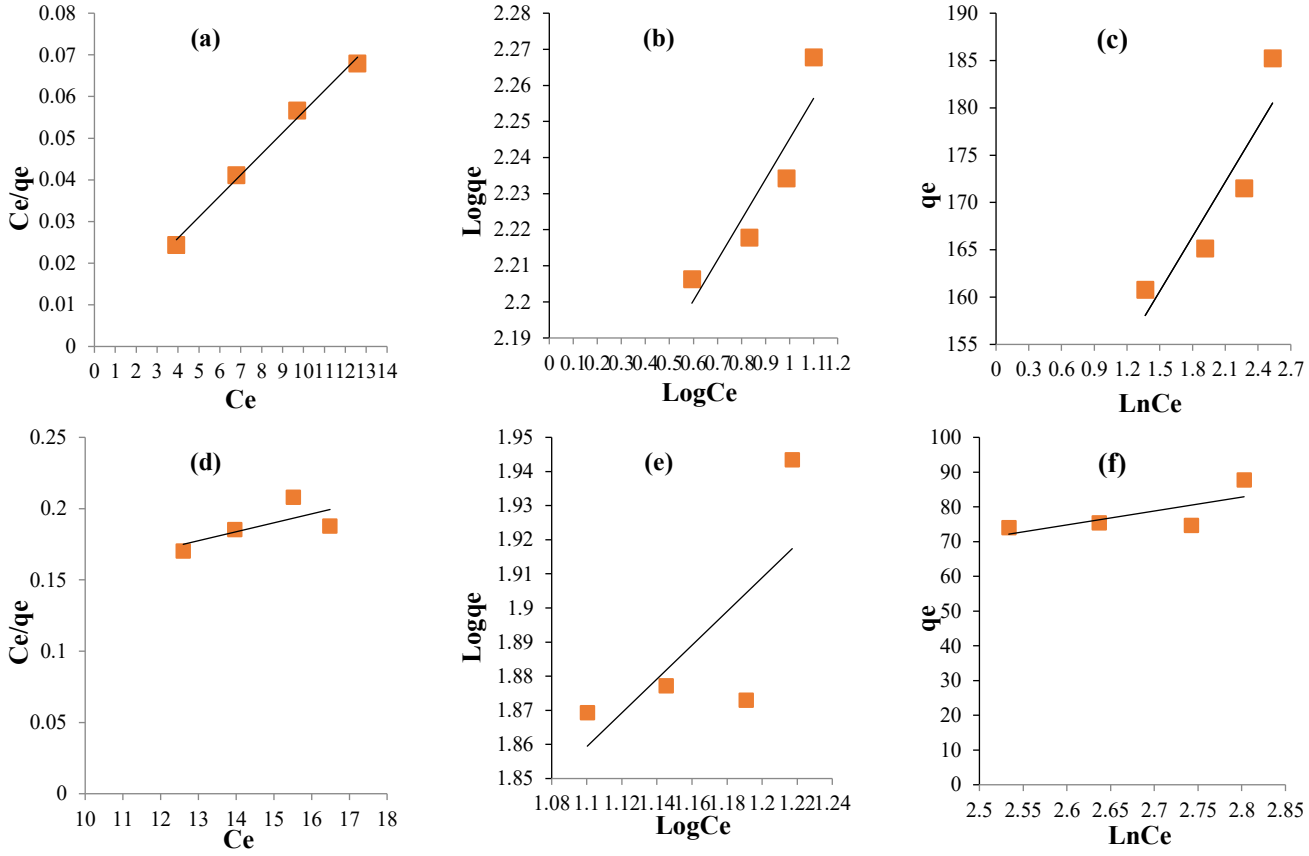


The results of fitting the experimental data to the equilibrium isotherms are presented in Table 3. According to Table 3a, the higher $R^2$ values indicate better correlation of the experimental data with the Langmuir isotherm model. The Langmuir results show that the adsorption of cationic methylene blue dye on the adsorbent occurs as a monolayer, with $R_L < 1$ indicating favorable adsorption. The maximum adsorption capacity ($Q_{max}$) of CMP-Et was found to be 200 mg/g, demonstrating its high specific surface area (Arami et al., 2005). The results of Basic Red 46 adsorption on CMP-Et (Table 3b) show relative agreement of the experimental data with both the Freundlich and Temkin isotherm models. The Freundlich

results (1/n < 1) indicate similarity to a normal Langmuir-type isotherm, while the Temkin results suggest that adsorption occurs partially through chemisorption(Mahmoodi et al. 2019).

**Table 3** The isotherm Langmuir, Freundlich, and Temkin data of a) MB and b) BR-46 adsorption (20 ppm) by CMP-Et metal-organic framework

| Isotherm | Equation | Plot | Parameters | Unit | a | b |
|---|---|---|---|---|---|---|
| | | | | | MB-20 (mg/l) | BR46-20 (mg/l) |
| Langmuir | $C_e/q_e=(1/K_L\ Q_{max})+(1/Q_{max})C_e$ <br> $R_L=1/(1+K_LC_0)$ | $C_e/q_e$ VS. $C_e$ | $Q_{max}$ | mg/g | 200 | 166.66667 |
| | | | $K_L$ | L/mg | 1 | 0.0631579 |
| | | | $R^2$ | - | 0.992 | 0.481 |
| | | | $R_L$ | - | 0.047619 | 0.4418605 |
| Freundlich | $Logq_e= LogK_F + (1/n)\ LogC_e$ | log $q_e$ VS. log $C_e$ | 1/n | - | 0.112 | 0.495 |
| | | | $K_F$ | L/mg | 135.83134 | 20.606299 |
| | | | $R^2$ | - | 0.843 | 0.522 |
| Temkin | $q_e= B_T\ LnK_T + B_T\ LnC_e$ | $q_e$ VS. ln $C_e$ | $B_T$ | - | 19.24 | 40 |
| | | | $K_T$ | L/mg | 939.28068 | 0.481909 |
| | | | $R^2$ | - | 0.829 | 0.519 |

**Table 4** Comparison of the adsorption performance of CMP-Et with various metal-organic frameworks for the removal of organic dyes from aqueous solutions

| Entry | Adsorbent | Adsorbate | Experimental Conditions | Adsorption capacity (mg/g) | Kinetic Model | Equilibrium Model | Ref. |
|---|---|---|---|---|---|---|---|
| 1 | MIL-53 | Methyl orange | T= 25-45 ºC<br>pH= 3-8.5<br>$C_0$= 30-40 ppm | 57.9 | Pseudo-Second-Order | Langmuir | Haque et al. 2010 |
| 2 | $NH_2$-MIL-101(Al) | Methylene blue[a]<br>Methyl orange[b] | T= 30-50 ºC<br>$C_0$= 20-40 ppm | 762 ± 12[a]<br>188±9[b] | Pseudo first-order[a]<br>Pseudo-Second-Order[b] | Langmuir | Haque et al. 2014 |
| 3 | MIL-101/ graphene Oxide | Amaranth[a]<br>sunset yellow[b]<br>Carmine[c] | pH= 7-12 | 111.01[a]<br>81.28[b]<br>77.61[c] | Pseudo-Second-Order | Freundlich | Li et al. 2016 |
| 4 | IFMC-1 | Methylene blue[a]<br>Basic red-46[b] | T= RT<br>pH= neutral | 293.9[a]<br>135.2[b] | Pseudo-Second-Order | Langmuir | Asadi et al. 2022b |
| 5 | Cr-BTC/SA-R[a]<br>Cr-BTC/SA-A[b] | Methylene blue | T= 25ºC<br>pH= 10<br>$C_0$= 10 ppm | 13.90[a]<br>10.06[b] | Pseudo-second-order | Temkin[a]<br>Langmuir and Freundlich[b] | Sonmez et al. 2024 |
| 6 | CMP-Et | Methylene blue[a]<br>Basic red-46[b] | T= RT<br>pH= natural<br>$C_0$= 20 ppm | 161[a]<br>74[b] | Pseudo-second-order | Langmuir[a]<br>Freundlich/ Temkin[b] | This work |

### 3.2.4 Comparison with Previously Reported MOFs

The adsorption performance of the metal-organic framework CMP-Et was compared with other MOF-based adsorbents (Table 4). Under ambient temperature and natural pH conditions, CMP-Et demonstrated adsorption capacities of 161 mg/g for MB and 74 mg/g for BR-46 at an initial concentration of 20 ppm. These results indicate competitive performance relative to established adsorbents: MIL-53 (57.9 mg/g for methyl orange; Haque et al. (2010)), $NH_2$-MIL-101(Al) (188 mg/g for methyl orange; Haque et al. (2014), and IFMC-1 (135.2 mg/g for Basic red-46; Asadi et al. (2022b). Kinetic analysis revealed that CMP-Et follows pseudo-second-order kinetics, consistent with benchmark MOFs (MIL-53, $NH_2$-MIL-101(Al), and IFMC-1). Equilibrium studies showed Langmuir model compliance for MB adsorption and Freundlich/Temkin model fits for BR-46, highlighting its adaptability to multiple adsorption mechanisms. These findings position CMP-Et as a versatile and efficient adsorbent for diverse aqueous-phase dye removal applications.

## 4. Conclusion

This study successfully developed an ethanol-based copper-melamine framework (CMP-Et) through solvent-mediated modification of the previously reported $[Cu(\eta^1\text{-}OAc)(\mu\text{-}OCH_3)(MA)]_2$ (CMP-Me) structure, and employed it for the investigation of cationic dye adsorption.

1. The metal-organic frameworks CMP-Me and CMP-Et MOFs were characterized using X-ray diffraction (XRD), Fourier-transform infrared spectroscopy (FTIR), and scanning electron microscopy (SEM) techniques.

2. The adsorption capacities of CMP-Et for cationic dyes MB and BR-46 were calculated as 161 and 74 mg/g, respectively. Results demonstrate that CMP-Et exhibits high adsorption capacity for cationic pollutants due to its three free $NH_2$ groups.

3. MB adsorption on CMP-Et followed the Langmuir isotherm and pseudo-second-order kinetics.

Although CMP-Et utilizes low-cost raw materials, the metal-ligand bonds may dissociate under high-temperature, strongly acidic, or alkaline conditions due to coordination bond weakening. To address this stability limitation, we propose post-synthetic modification of the MOF surface with carboxylate and sulfonate functional groups. This approach would not only enhance structural stability but also enable anionic pollutant adsorption. As an efficient and cost-effective adsorbent, CMP-Et exhibits significant potential for various industrial applications, including wastewater treatment, petrochemical processing, and the food industry, offering promising solutions for improving water quality and reducing environmental pollution.

## Statements and Declarations

### Acknowledgements

The authors express their gratitude to Eurasia Company, particularly Mr. Ali Ghorbani, for the financial support and collaboration that greatly facilitated this research. They also acknowledge Ardakan University for its institutional support.

### Data availability

The datasets generated and analyzed during this study are included in this published article.

### Conflicts of interest

The author of this paper declared no conflict of interest regarding the authorship or publication of this paper.

### Author contribution

**E. Asadi**: Investigation, Data Curation, Writing – Original Draft, Visualization, Revision; **F. Abyar**: Conceptualization, Methodology, Project Administration, Writing – Review & Editing; **F. Abrishami**: Supervision, Validation, Writing – Review & Editing.

### AI Use Declaration

This study did not incorporate artificial intelligence techniques; instead, all analyses and optimizations were conducted using conventional and widely accepted analytical methods.

### References

Aksu, Z., Ertuğrul, S., & Dönmez, G. (2010). Methylene Blue biosorption by Rhizopus arrhizus: Effect of SDS (sodium dodecylsulfate) surfactant on biosorption properties. *Chemical Engineering Journal,* 158(3), 474-481. https://doi.org/10.1016/j.cej.2010.01.029

Arami, M., Limaee, N. Y., Mahmoodi, N. M., & Tabrizi, N. S. (2005). Removal of dyes from colored textile wastewater by orange peel adsorbent: Equilibrium and kinetic studies. *Journal of Colloid and Interface Science*, *288*(2), 371-376. https://doi.org/10.1016/j.jcis.2005.03.020

Asadi, E., Bakherad, M., & Ghasemi, M. H. (2022a). High and selective adsorption of methylene blue using N-rich, microporous metal–organic framework $[ZnBT(H_2O)_2]_n$. *Journal of the Iranian Chemical Society*, *19*(1), 173-185. https://doi.org/10.1007/s13738-021-02297-7

Asadi, E., Abrishami, F., & Abyar, F. (2022b). Improvement strategies on metal–organic frameworks (IFMC-1) as adsorbent and its kinetic study for dye pollutant removal and wastewater treatment. *Journal of Coordination Chemistry*, *75*(19-24), 2771-2785. https://doi.org/10.1080/00958972.2022.2143268

Asadi, E., Bakherad, M., Ghasemi, M. H., Shakeri, A., & Nasrollahi, E. (2025). Innovative application of high nitrogen magnetic MOF as a catalyst in the aza-Michael reaction. *Journal of Porous Materials*, *32*, 1627-1645. https://doi.org/10.1007/s10934-025-01789-8

Ashraf, R. S., Abid, Z., Shahid, M., Rehman, Z. U., Muhammad, G., Altaf, M., & Raza, M. A. (2021). Methods for the treatment of wastewaters containing dyes and pigments. *Water Pollution and Remediation: Organic Pollutants*, 597-661. https://doi.org/10.1007/978-3-030-52395-4_17

Azhar, M. R., Abid, H. R., Sun, H., Periasamy, V., Tadé, M. O., & Wang, S. (2017). One-pot synthesis of binary metal organic frameworks (HKUST-1 and UiO-66) for enhanced adsorptive removal of water contaminants. *Journal of Colloid and Interface Science*, *490*, 685-694. https://doi.org/10.1016/j.jcis.2016.11.100

Azizian, S., & Eris, S. (2021). Adsorption isotherms and kinetics. *In Interface Science and Technology* (Vol. 33, pp. 445-509). Elsevier. https://doi.org/10.1016/B978-0-12-818805-7.00011-4

Brij, B. T., & Clint, O. T. (2010). Use of basic methylene blue dye for specific surface area measurement of metal hexacyanoferrate(II) complexes. *Revista de la Sociedad Químicadel Perú*, *76*(4), 330-335.

Bullen, J. C., Saleesongsom, S., Gallagher, K., & Weiss, D. J. (2021). A revised pseudo-second-order kinetic model for adsorption, sensitive to changes in adsorbate and adsorbent concentrations. *Langmuir*, *37*(10), 3189-3201. https://doi.org/10.1021/acs.langmuir.1c00142

Chen, C., Yeh, C.-W., & Chen, J.-D. (2006). Syntheses, structures and thermal properties of two new copper(II) melamine complexes. *Polyhedron*, *25*(6), 1307-1312. https://doi.org/10.1016/j.poly.2005.09.020

Değermenci, G. D., Değermenci, N., Ayvaoğlu, V., Durmaz, E., Çakır, D., & Akan, E. (2019). Adsorption of reactive dyes on lignocellulosic waste; characterization, equilibrium, kinetic and thermodynamic studies. *Journal of Cleaner Production*, *225*, 1220–1229. https://doi.org/10.1016/j.jclepro.2019.03.260

Deshmukh, S. M., Dhokpande, S. R., Sankhe, A., & Khandekar, A. (2025). Effluent wastewater technologies for textile industry: a review. *Review in Inorganic Chemistry*, *45*(1), 21-40. https://doi.org/10.1515/revic-2024-0046

Dharmarathna, S. P., & Priyantha, N. (2024). Investigation of boundary layer effect of intra-particle diffusion on methylene blue adsorption on activated carbon. *Energy Nexus*, *14*, 100294. https://doi.org/10.1016/j.nexus.2024.100294

Dhokpande, S. R., Deshmukh, S. M., Khandekar, A., & Sankhe, A. (2024). A review outlook on methods for removal of heavy metal ions from wastewater. *Separation and Purification Technology*, 127868. https://doi.org/10.1016/j.seppur.2024.127868

El Jery, A., Alawamleh, H. S. K., Sami, M. H., Abbas, H. A., Sammen, S. S., Ahsan, A., Imteaz, M., Shanableh, A., Shafiquzzaman, M., & Osman, H. (2024). Isotherms, kinetics and thermodynamic mechanism of methylene blue dye adsorption on synthesized activated carbon. *Scientific Reports*, 14(1), 970. https://doi.org/10.1038/s41598-024-55385-y

Fattahi, N., Fattahi, T., Kashif, M., Ramazani, A., & Jung, W.-K. (2024). Lignin: A valuable and promising bio-based absorbent for dye removal applications. *International Journal of Biological Macromolecules*, 133763. https://doi.org/10.1016/j.ijbiomac.2024.133763

Freund, R., Zaremba, O., Arnauts, G., Ameloot, R., Skorupskii, G., Dincă, M., Bavykina, A., Gascon, J., Ejsmont, A., & Goscianska, J. (2021). The current status of MOF and COF applications. *Angewandte Chemie*, *60*(45), 23975–24001. https://doi.org/10.1002/anie.202106259

Gangu, K. K., Maddila, S., Mukkamala, S. B., & Jonnalagadda, S. B. (2016). A review on contemporary metal–organic framework materials. *Inorganica Chim*ica Acta, *446*, 61-74. https://doi.org/10.1016/j.ica.2016.02.062

George, W. O., Has, T., Hossain, M. F., Jones, B. F., & Lewis, R. (1998). Hydrogen-bonded forms of ethanol—IR spectra and ab initio computations. *Journal of Chemical Society, Faraday Transactions*, *94*(18), 2701-2708. https://doi.org/10.1039/A803929A

Ghasemzadeh, R., & Naghavi, A. (2025). Water vapor adsorption in microporous and mesoporous frameworks for atmospheric water harvesting: Isotherms, kinetics, and thermodynamics insights. *SSRN*, https://doi.org/10.2139/ssrn.5227316

Hama Aziz, K. H., Fatah, N. M., & Muhammad, K. T. (2024). Advancements in application of modified biochar as a green and low-cost adsorbent for wastewater remediation from organic dyes. *Royal Society Open Science*, *11*(5), 232033. https://doi.org/10.1098/rsos.232033

Haque, E., Jun, J. W., & Jhung, S. H. (2011). Adsorptive removal of methyl orange and methylene blue from aqueous solution with a metal-organic framework material, iron terephthalate (MOF-235). *Journal of Hazardous Materials*, *185*(1), 507-511. https://doi.org/10.1016/j.jhazmat.2010.09.035

Haque, E., Lee, J. E., Jang, I. T., Hwang, Y. K., Chang, J.-S., Jegal, J., & Jhung, S. H. (2010). Adsorptive removal of methyl orange from aqueous solution with metal-organic frameworks, porous chromium-benzenedicarboxylates. *Journal of Hazardous Materials*, *181*(1–3), 535–542. https://doi.org/10.1016/j.jhazmat.2010.05.047

Haque, E., Lo, V., Minett, A. I., Harris, A. T., & Church, T. L. (2014). Dichotomous adsorption behaviour of dyes on an amino-functionalised metal–organic framework, amino-MIL-101 (Al). *Journal of Materials Chemistry A*, *2*(1), 193–203. https://doi.org/10.1039/C3TA13589F

He, Y., Tan, Y., & Zhang, J. (2014). An anionic MOF for separation of organic dyes via cationic-exchange and size-exclusion. *Acta Chimica Sinica*, *72*(12), 1228-1232. DOI: 10.6023/A14090632

Ho, Y.-S. (2006). Review of second-order models for adsorption systems. *Journal of Hazardous Materials*, *136*(3), 681–689. https://doi.org/10.1016/j.jhazmat.2005.12.043

Hor, K. Y., Chee, J. M. C., Chong, M. N., Jin, B., Saint, C., Poh, P. E., & Aryal, R. (2016). Evaluation of physicochemical methods in enhancing the adsorption performance of natural zeolite as low-cost adsorbent of methylene blue dye from wastewater. *Journal of Cleaner*

*Prod*uction, *118*, 197-209. https://doi.org/10.1016/j.jclepro.2016.01.056

Kaur, R., Kaur, A., Umar, A., Anderson, W. A., & Kansal, S. K. (2019). Metal organic framework (MOF) porous octahedral nanocrystals of Cu-BTC: Synthesis, properties and enhanced adsorption properties. *Materials Research Bulletin*, *109*, 124-133. https://doi.org/10.1016/j.materresbull.2018.07.025

Kestioğlu, K., Yonar, T., & Azbar, N. (2005). Feasibility of physico-chemical treatment and advanced oxidation processes (AOPs) as a means of pretreatment of olive mill effluent (OME). *Process Biochemistry*, *40*(7), 2409-2416. https://doi.org/10.1016/j.procbio.2004.09.015

Khamizov, R. K. (2020). A pseudo-second order kinetic equation for sorption processes. *Russian Journal of Physical Chemistry A, 94,* 171–176. https://doi.org/10.1134/S0036024420010148

Li, J.-J., Wang, C.-C., Fu, H.-f., Cui, J.-R., Xu, P., Guo, J., & Li, J.-R. (2017). High-performance adsorption and separation of anionic dyes in water using a chemically stable graphene-like metal–organic framework. *Dalton Transactions*, *46*(31), 10197-10201. https://doi.org/10.1039/C7DT02208E

Li, L., Shi, Z., Zhu, H., Hong, W., Xie, F., & Sun, K. (2016). Adsorption of azo dyes from aqueous solution by the hybrid MOFs/GO. *Water Science and Technology*, *73*(7), 1728–1737. https://doi.org/10.2166/wst.2016.009

Li, S., Huang, L., Guo, W., Feng, X., Cao, Y., & Liao, B. (2024). Two-dimensional copper-based metal-organic framework for efficient removal of methylene blue from wastewater. *European Journal of Inorganic Chemistry*, *27*(26), e202400240. https://doi.org/10.1002/ejic.202400240

Liu, H., Gao, G., Liu, J., Bao, F., Wei, Y., & Wang, H. (2019). Amide-functionalized ionic indium–organic frameworks for efficient separation of organic dyes based on diverse adsorption interactions. *CrystEngComm*, *21*(15), 2576-2584. https://doi.org/10.1039/C9CE00065H

Liu, X., Luo, J., Zhu, Y., Yang, Y., & Yang, S. (2015). Removal of methylene blue from aqueous solutions by an adsorbent based on metal-organic framework and polyoxometalate. *Journal of Alloys Compounds*, 648, 986-993. https://doi.org/10.1016/j.jallcom.2015.07.065

Mahmoodi, N. M., Oveisi, M., & Asadi, E. (2019). Synthesis of NENU metal-organic framework-graphene oxide nanocomposites and their pollutant removal ability from water using ultrasound. *Journal of Cleaner Production*, 211, 198-212. https://doi.org/10.1016/j.jclepro.2018.11.136

Majd, M. M., Kordzadeh-Kermani, V., Ghalandari, V., Askari, A., & Sillanpää, M. (2022). Adsorption isotherm models: A comprehensive and systematic review (2010− 2020). *Science of the Total Environment*, *812*, 151334. https://doi.org/10.1016/j.scitotenv.2021.151334

Moradi, O., & Panahandeh, S. (2022). Fabrication of different adsorbents based on zirconium oxide, graphene oxide, and dextrin for removal of green malachite dye from aqueous solutions. *Environmental Research*, *214*, 114042. https://doi.org/10.1016/j.envres.2022.114042

Lotha, T. N., Sorhie, V., Bharali, P., & Jamir, L. (2024). Advancement in sustainable wastewater treatment: A multifaceted approach to textile dye removal through physical, biological and chemical techniques. *Chemistry Select*, *9*(11), e202304093. https://doi.org/10.1002/slct.202304093

Namasivayam, C., Muniasamy, N., Gayatri, K., Rani, M., & Ranganathan, K. (1996). Removal of dyes from aqueous solutions by cellulosic waste orange peel. *Bioresource Technol*ogy, *57*(1), 37-43. https://doi.org/10.1016/0960-8524(96)00044-2

Oboh, I., Aluyor, E., & Audu, T. (2013). Second-order kinetic model for the adsorption of divalent metal ions on Sida acuta leaves. *International Journal of Physical Science*s, *8*(34), 1722–1728. https://doi.org/10.5897/IJPS09.146

Pascu, M., Pascu, D. E., Traistaru, G. A., Bunaciu, A. A., Orbeci, C., & Nechifor, A. C. (2013). Kinetic studies of some biological active extracts with antioxidant properties. *Review in Chemistry*, *64*, 785–790.

Qin, J.-S., Du, D.-Y., Li, W.-L., Zhang, J.-P., Li, S.-L., Su, Z.-M., Wang, X.-L., Xu, Q., Shao, K.-Z., & Lan, Y.-Q. (2012). N-rich zeolite-like metal–organic framework with sodalite topology: high $CO_2$ uptake, selective gas adsorption and efficient drug delivery. *Chemical Science*, *3*(6), 2114-2118. https://doi.org/10.1039/C2SC00017B

Qin, J. S., Zhang, S. R., Du, D. Y., Shen, P., Bao, S. J., Lan, Y. Q., & Su, Z. M. (2014). A microporous anionic metal–organic framework for sensing luminescence of lanthanide (III) ions and selective absorption of dyes by ionic exchange. *Chemistry-A European Journal*, *20*(19), 5625-5630. https://doi.org/10.1002/chem.201304480

Sharma, Y., Upadhyay, U. S., & Gode, F. (2009). Adsorptive removal of a basic dye from water and wastewater by activated carbon. *Journal of Applied Sciences in Environmental Sanitation*, 4, 21-24.

Sobhanardakani, S., Ghoochian, M., Jameh-Bozorghi, S., & Zandipak, R. (2017). Assessing of removal efficiency of indigo carmine from wastewater using MWCNTs. *Iranian Journal of Science and Technology, Transactions A: Science*, *41*, 1047-1053. https://doi.org/0.1007/s40995-017-0312-z

Sobhanardakani, S., Zandipak, R., Khoshsafar, H., & Zandipak, R. (2016). Removal of cationic dyes from aqueous solutions using $NiFe_2O_4$ nanoparticles. *Journal of Water Supply: Research and Technology—Aqua*, *65*(1), 64-74. https://doi.org/10.2166/aqua.2015.046

Sobhanardakani, S., Zandipak, R., & Sahraei, R. (2013). Removal of Janus Green dye from aqueous solutions using oxidized multi-walled carbon nanotubes. *Toxicological and Environmental Chemistry*, 95(6), pp.909-918. https://doi.org/10.1080/02772248.2013.840379

Sonmez, G., and Akyuz, L. (2024). In situ preparation and characterization of Cr-MOF-alginates for methylene blue through the adsorption process. *Journal of Water Process Engineering*, *62*, 105318. https://doi.org/10.1016/j.jwpe.2024.105318

Stavila, V., Talin, A. A., & Allendorf, M. D. (2014). MOF-based electronic and opto-electronic devices. *Chemical Society Reviews*, *43*(16), 5994-6010. https://doi.org/10.1039/C4CS00096J

Wang, C., Liu, X., Demir, N. K., Chen, J. P., & Li, K. (2016). Applications of water stable metal–organic frameworks. *Chemical Society Review*, *45*(18), 5107-5134. https://doi.org/10.1039/C6CS00362A

Yin, H., Qiu, P., Qian, Y., Kong, Z., Zheng, X., Tang, Z., & Guo, H. (2019). Textile wastewater treatment for water reuse: a case study. *Processes*, *7*(1), 34. https://doi.org/10.3390/pr7010034

Zandipak, R., & Sobhanardakani, S. (2016). Synthesis of $NiFe_2O_4$ nanoparticles for removal of anionic dyes from aqueous solution. *Desalination and Water Treatment*, *57*(24), 11348-11360. https://doi.org/10.1080/19443994.2015.1050701